Experimentally Realizable $\mathcal{PT}$ Phase Transitions in Reflectionless Quantum Scattering

Micheline B. Soley,[1,2,3,4] Carl M. Bender,[5] and A. Douglas Stone[3,6]
[1]Department of Chemistry, University of Wisconsin-Madison, 1101 University Avenue, Madison, Wisconsin 53706, USA
[2]Department of Physics, University of Wisconsin-Madison, 1150 University Avenue, Madison, Wisconsin 53706, USA
[3]Yale Quantum Institute, Yale University, PO Box 208334, New Haven, Connecticut 06520, USA
[4]Department of Chemistry, Yale University, 225 Prospect Street, New Haven, Connecticut 06520, USA
[5]Department of Physics, Washington University, St. Louis, Missouri 63130, USA
[6]Department of Applied Physics, Yale University, New Haven, Connecticut 06520, USA

(Received 3 November 2022; revised 24 March 2023; accepted 10 May 2023; published 22 June 2023)

Above-barrier quantum scattering with truncated real potentials $V(x) = -|x|^p$ provides an experimentally accessible platform that exhibits spontaneous parity-time symmetry breaking as p is varied. The unbroken phase has reflectionless states that correspond to bound states in the continuum of the nontruncated potentials at arbitrarily high discrete real energies. In the fully broken phase there are no bound states. There is a mixed phase in which exceptional points occur at specific energies and values of p. These effects should be observable in cold-atom scattering experiments.

DOI: 10.1103/PhysRevLett.130.250404

Two topics of wide and interdisciplinary interest are quantum and classical wave equations with complex potentials (or susceptibilities) that are symmetric under the product of parity and time reversal ($\mathcal{PT}$) and wave equations with real potentials (or susceptibilities) that support bound states in the continuum (BICs). In the former case one has the interesting feature of real spectra up to a symmetry-breaking transition despite the complex nature of the potential, and in the latter one has the feature of nondecaying localized states despite symmetry-allowed coupling to the scattering continuum. A limitation in realizing either $\mathcal{PT}$ systems or BICs exactly in quantum experiments is the lack of fundamental complex potentials in nature in the former case and the necessity of infinite-range forces or substrates in the latter. Building on recent work on reflectionless scattering, we show here that both of these limitations can be circumvented by studying above-barrier reflection of quantum particles from smooth, "upside-down," parity-symmetric, *real* potentials. First, the reflectionless boundary conditions make the problem non-Hermitian but $\mathcal{PT}$ symmetric, allowing a $\mathcal{PT}$ phase transition in the spectrum as the potential is varied. Second, each reflectionless state approximates a BIC in the scattering region, allowing one to straightforwardly probe the energies of the BICs and their wave functions in scattering experiments. We show that experiments testing both effects are feasible using atomic condensates and current atomic-trap technology.

For one-dimensional potentials, $\mathcal{PT}$ symmetry refers to Schrödinger equations and boundary conditions that map into themselves under combined $x \to -x$ and complex conjugation. This condition is less restrictive than the Hermiticity condition imposed in conventional quantum mechanics and allows for complex potentials with antisymmetric imaginary parts. Essentially all research on this topic has focused on Schrödinger equations with complex potentials or classical wave equations with complex susceptibility. Here, as noted, we treat physically realizable Schrödinger equations with potentials that have both $\mathcal{P}$ and $\mathcal{T}$ symmetry but, due to the reflectionless boundary conditions, the differential operator is non-Hermitian with only $\mathcal{PT}$ symmetry.

There have been relatively few experimental demonstrations of phenomena related to $\mathcal{PT}$ symmetry in quantum mechanics because quantum potentials are real in the absence of reservoir coupling. Such experiments have thus been restricted to open systems coupled to reservoirs that are treated statistically and introduce phenomenological imaginary terms into the Schrödinger equation [1–6] or have relied on postselection of data that can mimic the effect of loss [7–9]. In contrast, there has been an intensive experimental study of $\mathcal{PT}$ symmetry and its breaking in systems described by classical wave equations, where imaginary terms representing loss and gain are also introduced into the equations to describe coupling to reservoirs, but these tend to be more controllable and relatively easy to fabricate and measure. Examples span classical electromagnetism [10–15], acoustics [16,17], electronics [18–21], and mechanical systems [22]. In several cases these classical $\mathcal{PT}$-symmetric systems have shown potential utility for applications in laser technology [23,24], sensing [25,26], and wireless power transfer [27,28].

Our work builds off the work in Refs. [29,30], which studied $\mathcal{PT}$-symmetry phenomena in a class of nonrelativistic quantum systems with complex potentials of the

form $V(x) = x^2(ix)^\epsilon$ and $V(x) = x^4(ix)^\epsilon$ (ϵ real), which satisfy the $\mathcal{PT}$-symmetry condition. Importantly, for various choices of even integers ϵ these potentials lead to purely real upside-down $\mathcal{PT}$-symmetric potentials of the form $V(x) = -x^2, -x^4, -x^6, -x^8, \ldots$. It was shown that for these real potentials with even integer power $p \geq 4$ there exist discrete weakly bound states for real energies $E_i > 0$, but for $p = 2$ there are no real-energy solutions, nonreal-energy solutions. It was realized that real-energy solutions correspond to reflectionless states [31], although due to the unbounded-below nature of the potentials, the particles are not approximately freely propagating at $\pm\infty$, which invalidates the assumptions of standard scattering theory. The current work proposes a means to probe this quantum physics in an experimentally realizable setup.

We show that the reflectionless states of a continuous class of *truncated* upside-down real potentials, distinct from those considered previously, show all the characteristics of $\mathcal{PT}$-symmetric systems: specifically, the presence of unbroken, mixed, and broken phases and spontaneous symmetry-breaking transitions at exceptional points (EPs), despite the absence of imaginary terms in the potential. We detect the signature of the weakly bound BICs above such potentials with energies given precisely by those predicted for the unbounded-below integer cases considered in Ref. [32]. This constitutes the first theoretical prediction of such $\mathcal{PT}$-symmetry phenomena in an experimentally realizable quantum system described fully by Schrödinger's equation.

We consider potentials of the form $V(x) = -|x|^p$ for $p \in \mathbb{R}$, truncated to constant energy outside of the domain $-L \leq x \leq L$ [see Fig. 1(a)]. [We consider energy truncation in Sec. IV of the Supplemental Material (SM) and obtain similar results [33].] Unlike the potentials studied in Refs. [29,30], these potentials are real and parity symmetric for all p but nonanalytic at the origin (except at even integer p values). For convenience we smooth the potential to make it continuously differentiable at the truncation point by introducing a potential $V(x, w)$, where the real parameter w determines the sharpness of the truncation (see Sec. II A of the Supplemental Material [33]). Motivated by a different truncation of the unbounded upside-down potentials used in Ref. [32], we present a qualitatively different approach that replaces those potentials with real potentials having odd and noninteger powers p. We also consider a standard scattering geometry for which the potential goes smoothly to zero in the asymptotic region. Their nonanalytic behavior distinguishes this class of real potentials from the analytic complex potentials studied in Refs. [29,30], which can be continued in the complex plane. The potential $V(x) = -|x|^p$ cannot be continued in x, although $V(x)$ and its eigenvalues are analytic in p.

We first verify that the reflectionless states of these truncated $V(x) = -V_0|x|^p$ potentials obey $\mathcal{PT}$ symmetry. We introduce V_0 here to clarify the choice of units. Since the potential is real, it is both $\mathcal{P}$ and $\mathcal{T}$ symmetric, and the problem superficially appears to be Hermitian; however, we now investigate the effect of the reflectionless boundary conditions. The 1D Schrödinger equation is

$$0 = -\frac{\hbar^2}{2m}\phi''(x) + [V(x) - E]\phi(x),$$

where m is the mass of the relevant quantum particle. Measuring E from the top of the barrier, we introduce the length scale $x_0 \equiv (E/V_0)^{1/p}$, where, for values of p for which the infinite potential has bound states, we choose the ground-state energy $E = E_0$. Henceforth, x denotes the position in units of x_0 leading to $V(x) = -E_0|x|^p$; finally, we take energy units with $E_0 = 1$ to recover $V(x) = -|x|^p$. (In the case of no bound states E can be chosen arbitrarily.) Assuming that the potential and kinetic energy are of the same order and hence of order E_0, we find that $x_0 \sim (h^2/mV_0)^{1/(p+2)}$, $E_0 \sim V_0 x_0^p \sim (h^2/m)^{(p/(p+2))} V_0^{(2/(p+2))}$. Now we look for a solution with a right-moving

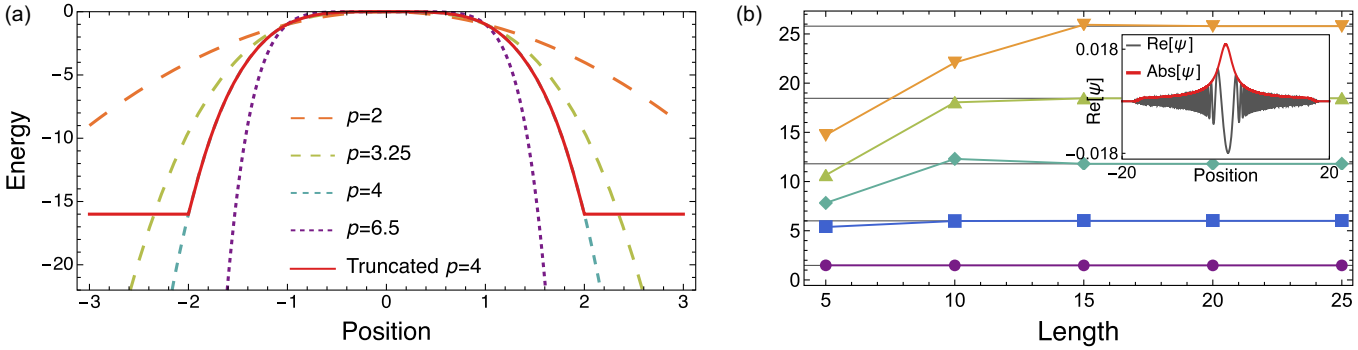

FIG. 1. (a) Upside-down potential $V(x) = -x^4$ (dashed blue line combined with the curving bold red line) is one of a class of real potentials $V(x) = -|x|^p$ for $p \in \mathbb{R}$ (dashed multicolor lines). Red line shows the truncated potential for $p = 4$, length $L = 2$, and smoothing $w = 1000$. (b) Reflectionless scattering mode spectra of the truncated $-x^4$ potential are real and converge with increasing L to the exact weakly-bound-state energies E_i of the nontruncated potential (gray lines, $i = 0$–4 shown). Inset: scattering wave function for $E = E_0$ RSM of the truncated $V(x) = -x^4$ potential (gray line, Re$[\psi]$; thick red line, $|\psi|^2$) with predicted $|1/x|$ decay.

wave only, which satisfies the reflectionless boundary conditions

$$\phi'(-L) \sim ik\phi(-L), \qquad \phi'(L) \sim ik\phi(L) \quad (w \to 0),$$

where $k \equiv \sqrt{2m(E+V_b)/\hbar}$, where $V_b = |V(\pm L)|$ is the barrier height. These conditions map into left-moving waves under either $\mathcal{P}$ or $\mathcal{T}$ separately, but map back into themselves under the product of $\mathcal{P}$ and $\mathcal{T}$. An implication of the $\mathcal{PT}$ symmetry is that any reflectionless solutions either must have a real energy or must occur in complex-conjugate pairs. If the former holds, the $\mathcal{PT}$ symmetry is said to be *unbroken*; if the latter holds, it is *broken*. If both types of solutions exist for a given p, the spectrum is mixed. Solutions with broken $\mathcal{PT}$ symmetry do not yield reflectionless states.

For the infinite-length and depth potentials studied in Ref. [30], the real solutions are BICs, peaked at the origin and decaying weakly [$\phi(x) \sim 1/x$ as $x \to \pm\infty$ for the case $p = 4$]. The striking finding was that an upside-down, *repulsive* potential can nonetheless create bound quantum states, albeit weakly bound. This contrasts strongly with the standard exponentially decaying bound states of attractive real potentials. For the finite potentials (after truncation) considered here, we have a scattering geometry, and the reflectionless above-barrier states propagate as plane waves at infinity and are not square integrable. A recent general theory of reflectionless scattering modes (RSMs) [42,43] predicts an infinite set of discrete reflectionless solutions for generic potentials with $\mathcal{PT}$ symmetry that also occur at real energies or in complex-conjugate pairs. The hypothesis behind the current work is that the RSMs of these truncated potentials will exhibit a resonant peak in space near the top of the barrier with the same spatial profile as the BICs of the unbounded potentials and at nearly the same energy.

To test this hypothesis, we apply RSM theory to quantum mechanics. Until now this theory has been applied to electromagnetic or optical systems [42,43], but the method is general and can be applied to quantum-scattering systems in any number of dimensions. We derive a specifically quantum formalism for the RSM theory in Sec. III of the SM [33]. An attractive feature of the theory is that it calculates directly the discrete complex spectrum of reflectionless energies (referred to as R-zeros). One need not solve the scattering problem and search for zero reflection. The R-zero spectrum is similar but distinct from the more familiar spectrum of complex-energy resonances, which satisfy purely outgoing boundary conditions.

General RSM theory simplifies for the current case of a 1D (two-channel) geometry, and the reflectionless energies can be found by a simple modification of the method of perfectly matched layers (also referred to as complex scaling [44] or as complex absorbing potentials [45]), which we use here. Real-energy solutions correspond to steady-state harmonic scattering and thus imply a zero of the reflection coefficient at the calculated input energy. Complex-energy solutions do not give zero reflection under uniform harmonic excitation but, if the R-zero is isolated and near the real axis, it will be detectable via a narrow dip in the reflection below the background, near the real part of its energy. Hence we can study these R-zero spectra and the corresponding eigenfunctions for the truncated potentials and compare their properties to the unbounded potentials studied previously. We find striking agreement between the two systems.

As shown in Fig. 1(b) and Sec. IV of the SM [33], the low-energy RSM energies for $p = 4$ are real and agree with the bound-state energies found for the infinite system with 7–8 digits of accuracy for sufficiently large L. Even for the shortest truncation length L considered, the ground-state energy is accurately found, and higher eigenenergies converge to known infinite-system values with increasing length L. Once the incident energies are known, these results are easily tested and confirmed by quantum-scattering calculations, as shown in Fig. 2 and in Secs. I and V of the SM [33]. Similar convergence is found with results obtained by energy truncation at $|V_{\max}|$ (see Sec. IV of the SM [33]).

Not only are the energies accurately predicted [32], but also the eigenfunctions in the interaction region perfectly

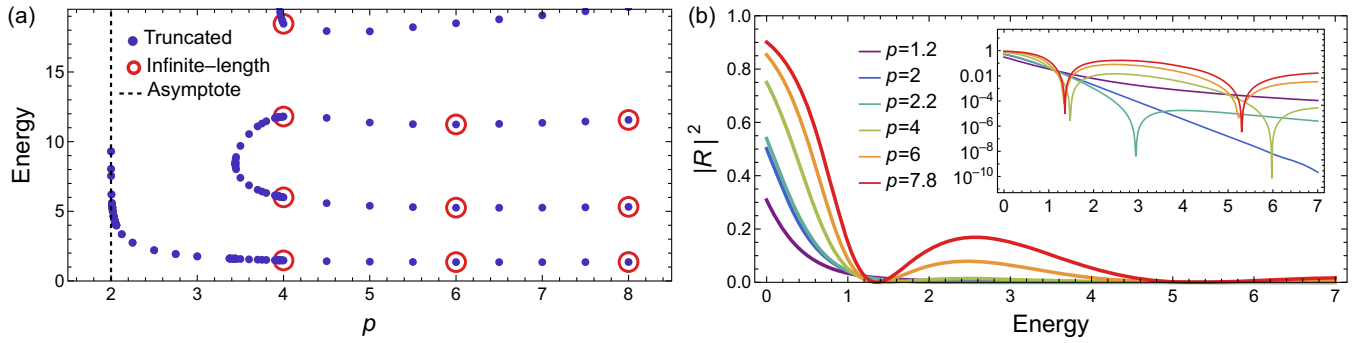

FIG. 2. (a) RSM spectrum of the class of truncated $V(x) = -|x|^p$ potentials, showing that the lower-energy RSMs agree closely with the known energies of the weakly bound states of the infinite-length potentials for even p (red circles), and (b) reflection coefficient calculations for the same, showing nonmonotonic behavior for $p > 2$ and deep dips toward zero (inset).

mimic the behavior predicted for the infinite system, as shown in the inset of Fig. 1(b). The eigenfunctions are symmetric around the origin and exhibit the predicted $|1/x|$ decay with three-digit accuracy. Thus, the intriguing weakly bound BICs of the infinite potential are directly observable in the truncated system. Note the rapid increase in the spatial oscillation frequency of the eigenfunction as the particle accelerates toward the asymptotic region, where the force vanishes.

RSM theory also allows us to search for a $\mathcal{PT}$ quantum phase transition within the class of potentials $V(x) = -|x|^p$ as p is varied, a phenomenon suggested by the earlier work on complex $\mathcal{PT}$ potentials cited above [29,30]. In Fig. 2(a) we plot the low-lying real-energy eigenvalues of this class of potential as p is varied between $2 \leq p \leq 8$. The $\mathcal{PT}$ symmetry and analyticity of the eigenvalues implies that as p is varied, eigenvalues cannot disappear or individually move into the complex plane, but can meet at certain parameter values and then, generically, move into the complex plane as conjugate pairs. These degeneracy points are the exceptional points, at which eigenvectors also coalesce, a non-Hermitian phenomenon. We find that for $p \geq 4$ there are only eigenvalues at real energies up to a high energy, above which the effect of our truncation becomes visible. This indicates that the behavior found for the infinite system at the discrete integers $p = 4$, 6, 8 (infinite number of real-energy bound states) is generic and continuous in p.

In the interval $2 < p < 4$ we see a series of EPs, which occur at higher p for higher energies; after the EPs, the eigenvalues separate and become complex-conjugate pairs. We only plot real energies, but in Sec. VI of the SM we show the full evolution in the complex plane [33]. For much of the interval $2 < p < 4$ there is only a single real RSM; above $p \approx 3.44$ a finite number of pairs of real reflectionless energies appear, emerging from the EPs. This corresponds to a partially broken $\mathcal{PT}$-symmetry phase, similar but distinct from the behavior of the real eigenenergies of the complex potentials studied in Ref. [30]. Finally, for $p \leq 2$, there are *no* real reflectionless energies (the unpaired ground states are pushed up to infinity at $p = 2$). This monotonically decreasing, nonresonant scattering behavior above the inverted harmonic potential has been known since the early days of quantum mechanics [46]. Our results show that the behavior changes qualitatively for any sharper polynomial barrier, and it is only the regime $p \leq 2$ that has fully broken $\mathcal{PT}$ symmetry.

Quantum-scattering results shown in Fig. 2(b) dramatically confirm the identification of a distinct transition between the fully broken $\mathcal{PT}$ phase ($p \leq 2$) and the partially broken phase ($2 < p \leq 4$). Up to $p = 2$, we see a slower than exponential, but monotonic, decay of the reflection coefficient as a function of energy. At $p = 2$, the asymptotic decay is exponential, and above it the decay is nonmonotonic with deep dips at the predicted reflection zeros (resolved only to a finite depth). However, as predicted by the RSM spectra in Fig. 2(a), for $p = 2.2$ there is only one such dip compared to $p \geq 4$ where there are many. Note also that the peak reflection for $p = 6$, *after* the first zero, has a reflection coefficient of ≈ 0.08, which should be measurable in experiments.

In this mixed regime the potential is still quite smooth and the above-barrier scattering is weak, making detection of the EPs challenging. If there is sufficient accuracy in measuring the reflection ($\sim 10^{-3} - 10^{-4}$), the approach to the EP at $p \approx 3.44$ can be detected by varying p in the interval $3.2 > p > 3.8$ and observing the merger of the two reflection dips around $p = 3.4$ (Fig. 3, inset). A signature of the EP that is currently too difficult to observe is the quartic line shape near the zero, predicted by the general RSM theory [42,47]; this effect is confirmed by our quantum calculations [see SM, Fig. 9(c) [33]].

To analyze further how the physics changes with the shape of the potential, we employ an approach to identify the origin of above-barrier reflection, which we call WKB *force* analysis. This method has been used previously to improve the accuracy of calculations of above-barrier reflection [48] and other quantum simulations [49]. Here we use the technique to determine the spatial origin of above-barrier reflection in these quantum potentials and the effect of truncation.

The method begins by observing that WKB wave functions, although approximate solutions of the Schrödinger equation, cannot capture above-barrier reflection in 1D. Starting with a positive momentum solution at $-\infty$, the local WKB momentum $p(x, E) \equiv \sqrt{2m[E - V(x)]}$ can never change sign if $E > V_{\max}$. In addition, it can be shown that given a potential $V(x)$, the WKB wave functions *exactly* satisfy a Schrödinger equation to which,

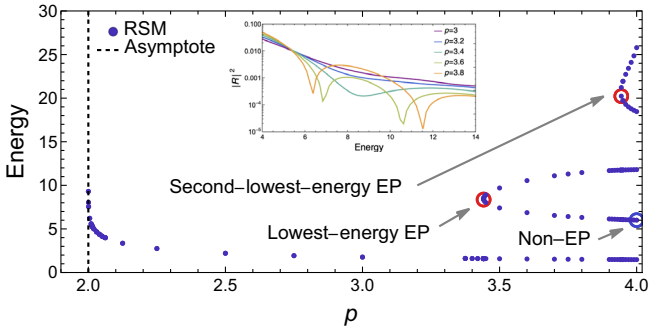

FIG. 3. $\mathcal{PT}$-symmetry transitions at exceptional points in the RSM spectrum for $p \approx 3.44, E_{\mathrm{EP}} = 8.4$ and $p \approx 3.94, E_{\mathrm{EP}} = 20.2$. Inset shows that the scattering near these EPs indicates coalescence of two RSMs as shape of the potential is varied ($p = 3.8$, yellow line; $p = 3.6$, olive line) into a single EP and R-zero ($p = 3.4$, teal line; $p = 3.2$, blue line; $p = 3$, purple line) at a reflection coefficient of order $\sim 10^{-4}$.

in addition to $V(x)$, one adds an energy-dependent potential correction $V_{\mathrm{WKB}}(x,E)$ of order $\hbar^2$ of the form

$$V_{\mathrm{WKB}}(x,E) = -\hbar^2\left[\frac{5}{32m}\left(\frac{V'(x)}{E-V(x)}\right)^2 + \frac{V''(x)}{8m[E-V(x)]}\right].$$

If we employ the reflectionless WKB states in the actual potential $V(x)$ to calculate above-barrier reflection using the Born approximation, the reflection from the potential $V(x)$ at energy E arises solely from the additional scattering induced by $V_{\mathrm{WKB}}(x,E)$. Thus, $V_{\mathrm{WKB}}(x,E)$ reveals the spatial location of above-barrier scattering; V_{WKB} is localized in a region around the potential maximum and vanishes far from the origin as $1/x^2$, even if $V(x)$ extends to infinity; thus, it can be used to analyze both the unbounded potentials $V(x) = -|x|^p$ and their truncated versions.

First, we calculate $V_{\mathrm{WKB}}(x,E)$ for upside-down infinite-length potentials. We study the shape of $V_{\mathrm{WKB}}(x,E,p)$ as p varies with $E = 1.477$ (the ground state for $p = 4$). As shown in Fig. 4 and Sec. VII of the SM [33], there is a qualitative change in V_{WKB} with p, and this change is insensitive to the value of E. For $p \leq 2$, V_{WKB} has a single peak at the origin, which is divergent due to nonanalytic behavior at the origin for $p < 2$. This is because V_{WKB} depends on V' and V'', at least one of which diverges for $p < 2$. At $p = 2$, $V(x)$ is analytic and for small x the peak of V_{WKB} is an inverted parabola. However, for $p > 2$, the peak splits into two peaks, symmetrically displaced from the origin, creating a small central well in V_{WKB}; this well becomes deeper as $p \to 4$, where it creates an approximately parabolic "trap." This is the signature of the quantum phase transition. For $p > 4$, the trap gets flatter at the center, making the scattering more localized at $x \approx \pm 1$, while $V(x)$ itself tends to a (semi-infinite in height) square-well potential, which has an infinite set of reflectionless above-barrier resonances.

In Sec. VII of the SM, we show the same analysis of $V_{\mathrm{WKB}}(x,E)$ for the truncated potential; the qualitative change in the shape in the central region is completely unchanged; additional spikes are seen away from the central region due to the truncation, but these spikes decrease as the truncation length increases [33].

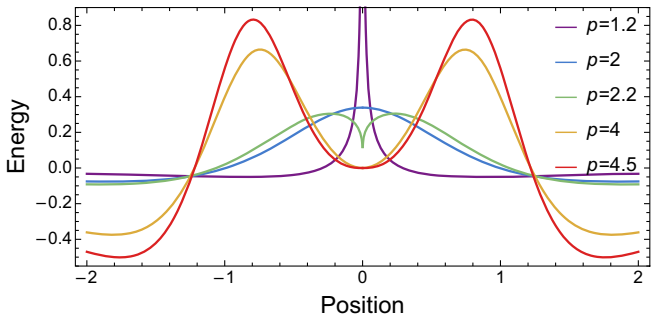

FIG. 4. WKB force analysis potential at $E = 1.477$ for the $V(x) = -|x|^p$ potential as a function of p, which indicates a quantum phase transition in reflection at $p = 2$ (solid blue line), in accordance with the quantum-scattering results and reflectionless scattering mode spectra.

In summary, quantum above-barrier scattering experiments in real "upside-down" potentials bring the physics of weakly bound BICs and the $\mathcal{PT}$-symmetry-breaking phase transition within reach of experimental observation. An exciting candidate for realizing such experiments is the scattering of condensates off of laser-engineered optical potentials. Similar experiments have already been reported [50,51], where a potential barrier of order 100 nK in height and several micrometers in length has been probed by a condensate of alkali atoms with energy width 1 nK [52] generated by techniques such as rapidly scanned lasers [53], digital micromirror devices [54,55], intensity masks [56], and holographic methods [57–60]. The qualitative features of the reflection spectra we predict are shown in Sec. I of the SM to be robust to smooth changes in the potential [33]; hence these phenomena will be relatively insensitive to experimental nonidealities in creating the potential as long as the leading term near the maximum is approximately correct. A particularly robust feature is the presence of a ground-state BIC or RSM with E_0 only weakly varying for $p \geq 4$. In Sec. I of the SM [33] we discuss this further and show that as p is varied between $p = 4$, 6, 7.8 the secondary peak in the reflection after the RSM varies from ~2% to 17%, an effect that should be observable in experiments. Given the ubiquity of quantum reflection in near-threshold quantum systems, the occurrence of such phenomena may not be limited to the $V(x) = -|x|^p$ potentials, but instead may be present in a wide range of quantum systems and could be relevant to such technologies as quantum sensing.

We thank E. J. Heller for stimulating conversations and N. Mantella, A. M. Steinberg, and N. Navon for helpful discussions. M. B. S. acknowledges financial support from the Yale Quantum Institute Postdoctoral Fellowship. Support for this research was provided by the Office of the Vice Chancellor for Research and Graduate Education at the University of Wisconsin-Madison with funding from the Wisconsin Alumni Research Foundation. A. D. S. and C. M. B. acknowledge financial support from the Simons Collaboration on Extreme Wave Phenomena Based on Symmetries. C. M. B. also acknowledges financial support from the Alexander von Humboldt Foundation and from the UK Engineering and Physical Sciences Research Council (EPSRC) grant at King's College London.

[1] K. F. Zhao, M. Schaden, and Z. Wu, Enhanced magnetic resonance signal of spin-polarized Rb atoms near surfaces of coated cells, Phys. Rev. A **81**, 042903 (2010).

[2] S. Bittner, B. Dietz, U. Günther, H. L. Harney, M. Miski-Oglu, A. Richter, and F. Schäfer, $\mathcal{PT}$ Symmetry and

Spontaneous Symmetry Breaking in a Microwave Billiard, Phys. Rev. Lett. **108**, 024101 (2012).
[3] C. Zheng, L. Hao, and G. L. Long, Observation of a fast evolution in a parity-time-symmetric system, Phil. Trans. R. Soc. A **371**, 20120053 (2013).
[4] J. Li, A. K. Harter, J. Liu, L. de Melo, Y. N. Joglekar, and L. Luo, Observation of parity-time symmetry breaking transitions in a dissipative Floquet system of ultracold atoms, Nat. Commun. **10**, 855 (2019).
[5] L. Ding, K. Shi, Q. Zhang, D. Shen, X. Zhang, and W. Zhang, Experimental Determination of $\mathcal{PT}$-Symmetric Exceptional Points in a Single Trapped Ion, Phys. Rev. Lett. **126**, 083604 (2021).
[6] Z. Ren, D. Liu, E. Zhao, C. He, K. K. Pak, J. Li, and G.-B. Jo, Chiral control of quantum states in non-Hermitian spin–orbit-coupled fermions, Nat. Phys. **18**, 385 (2022).
[7] M. Naghiloo, M. Abbasi, Y. N. Joglekar, and K. Murch, Quantum state tomography across the exceptional point in a single dissipative qubit, Nat. Phys. **15**, 1232 (2019).
[8] Y. Wu, W. Liu, J. Geng, X. Song, X. Ye, C.-K. Duan, X. Rong, and J. Du, Observation of parity-time symmetry breaking in a single-spin system, Science **364**, 878 (2019).
[9] W. Liu, Y. Wu, C.-K. Duan, X. Rong, and J. Du, Dynamically Encircling an Exceptional Point in a Real Quantum System, Phys. Rev. Lett. **126**, 170506 (2021).
[10] A. Guo, G. J. Salamo, D. Duchesne, R. Morandotti, M. Volatier-Ravat, V. Aimez, G. A. Siviloglou, and D. N. Christodoulides, Observation of $\mathcal{PT}$-Symmetry Breaking in Complex Optical Potentials, Phys. Rev. Lett. **103**, 093902 (2009).
[11] C. E. Rüter, K. G. Makris, R. El-Ganainy, D. N. Christodoulides, M. Segev, and D. Kip, Observation of parity–time symmetry in optics, Nat. Phys. **6**, 192 (2010).
[12] L. Feng, M. Ayache, J. Huang, Y.-L. Xu, M.-H. Lu, Y.-F. Chen, Y. Fainman, and A. Scherer, Nonreciprocal light propagation in a silicon photonic circuit, Science **333**, 729 (2011).
[13] A. Regensburger, C. Bersch, M.-A. Miri, G. Onishchukov, D. N. Christodoulides, and U. Peschel, Parity–time synthetic photonic lattices, Nature (London) **488**, 167 (2012).
[14] L. Xiao, T. Deng, K. Wang, Z. Wang, W. Yi, and P. Xue, Observation of Non-Bloch Parity-Time Symmetry and Exceptional Points, Phys. Rev. Lett. **126**, 230402 (2021).
[15] B. Peng, Ş. K. Özdemir, F. Lei, F. Monifi, M. Gianfreda, G. L. Long, S. Fan, F. Nori, C. M. Bender, and L. Yang, Parity–time-symmetric whispering-gallery microcavities, Nat. Phys. **10**, 394 (2014).
[16] C. Shi, M. Dubois, Y. Chen, L. Cheng, H. Ramezani, Y. Wang, and X. Zhang, Accessing the exceptional points of parity-time symmetric acoustics, Nat. Commun. **7**, 1 (2016).
[17] Y. Aurégan and V. Pagneux, $\mathcal{PT}$-Symmetric Scattering in Flow Duct Acoustics, Phys. Rev. Lett. **118**, 174301 (2017).
[18] N. M. Chtchelkatchev, A. A. Golubov, T. I. Baturina, and V. M. Vinokur, Stimulation of the Fluctuation Superconductivity by $\mathcal{PT}$ Symmetry, Phys. Rev. Lett. **109**, 150405 (2012).
[19] J. Schindler, A. Li, M. C. Zheng, F. M. Ellis, and T. Kottos, Experimental study of active LRC circuits with $\mathcal{PT}$ symmetries, Phys. Rev. A **84**, 040101(R) (2011).
[20] N. Bender, S. Factor, J. D. Bodyfelt, H. Ramezani, D. N. Christodoulides, F. M. Ellis, and T. Kottos, Observation of Asymmetric Transport in Structures with Active Nonlinearities, Phys. Rev. Lett. **110**, 234101 (2013).
[21] W. Cao, C. Wang, W. Chen, S. Hu, H. Wang, L. Yang, and X. Zhang, Fully integrated parity—time-symmetric electronics, Nat. Nanotechnol. **17**, 262 (2022).
[22] C. M. Bender, B. K. Berntson, D. Parker, and E. Samuel, Observation of $\mathcal{PT}$ phase transition in a simple mechanical system, Am. J. Phys. **81**, 173 (2013).
[23] L. Feng, Z. J. Wong, R.-M. Ma, Y. Wang, and X. Zhang, Single-mode laser by parity-time symmetry breaking, Science **346**, 972 (2014).
[24] H. Hodaei, M.-A. Miri, M. Heinrich, D. N. Christodoulides, and M. Khajavikhan, Parity-time–symmetric microring lasers, Science **346**, 975 (2014).
[25] P.-Y. Chen and J. Jung, $\mathcal{PT}$ symmetry and singularity-enhanced sensing based on photoexcited graphene metasurfaces, Phys. Rev. Appl. **5**, 064018 (2016).
[26] Z.-P. Liu, J. Zhang, Ş. K. Özdemir, B. Peng, H. Jing, X.-Y. Lü, C.-W. Li, L. Yang, F. Nori, and Y.-x. Liu, Metrology with $\mathcal{PT}$-Symmetric Cavities: Enhanced Sensitivity near the $\mathcal{PT}$-Phase Transition, Phys. Rev. Lett. **117**, 110802 (2016).
[27] S. Assawaworrarit, X. Yu, and S. Fan, Robust wireless power transfer using a nonlinear parity–time-symmetric circuit, Nature (London) **546**, 387 (2017).
[28] S. Assawaworrarit and S. Fan, Robust and efficient wireless power transfer using a switch-mode implementation of a nonlinear parity–time symmetric circuit, Nat. Electron. **3**, 273 (2020).
[29] C. M. Bender and S. Boettcher, Real Spectra in Non-Hermitian Hamiltonians Having $\mathcal{PT}$ Symmetry, Phys. Rev. Lett. **80**, 5243 (1998).
[30] C. M. Bender, Making sense of non-Hermitian Hamiltonians, Rep. Prog. Phys. **70**, 947 (2007).
[31] Z. Ahmed, C. M. Bender, and M. V. Berry, Reflectionless potentials and $\mathcal{PT}$ symmetry, J. Phys. A **38**, L627 (2005).
[32] C. M. Bender and M. Gianfreda, Scattering off $\mathcal{PT}$-symmetric upside-down potentials, Phys. Rev. A **98**, 052118 (2018).
[33] See Supplemental Material at http://link.aps.org/supplemental/10.1103/PhysRevLett.130.250404 for detailed methods and results, which includes Refs. [34–41].
[34] C. M. Bender, K. A. Milton, S. S. Pinsky, and L. Simmons, Jr., A new perturbative approach to nonlinear problems, J. Math. Phys. (N.Y.) **30**, 1447 (1989).
[35] R. E. Hamam, A. Karalis, J. D. Joannopoulos, and M. Soljačić, Coupled-mode theory for general free-space resonant scattering of waves, Phys. Rev. A **75**, 053801 (2007).
[36] J. D. Joannopoulos, S. G. Johnson, J. N. Winn, and R. D. Meade, *Photonic Crystals: Molding the Flow of Light*, 2nd ed. (Princeton University, Princeton, NJ, 2008).
[37] S. Fan, W. Suh, and J. D. Joannopoulos, Temporal coupled-mode theory for the Fano resonance in optical resonators, J. Opt. Soc. Am. A **20**, 569 (2003).
[38] W. Suh, Z. Wang, and S. Fan, Temporal coupled-mode theory and the presence of non-orthogonal modes in lossless multimode cavities, IEEE J. Quantum Electron. **40**, 1511 (2004).

[39] A. M. Lane and R. G. Thomas, R-matrix theory of nuclear reactions, Rev. Mod. Phys. **30**, 257 (1958).
[40] L. C. Leal, Brief review of the R-matrix theory, technical report, Oak Ridge National Laboratory, MIT Course, (2009).
[41] W. W. Hager, Updating the inverse of a matrix, SIAM Rev. **31**, 221 (1989).
[42] W. R. Sweeney, C. W. Hsu, and A. D. Stone, Theory of reflectionless scattering modes, Phys. Rev. A **102**, 063511 (2020).
[43] A. D. Stone, W. R. Sweeney, C. W. Hsu, K. Wisal, and Z. Wang, Reflectionless excitation of arbitrary photonic structures: A general theory, Nanophotonics **10**, 343 (2021).
[44] N. Moiseyev, Quantum theory of resonances: calculating energies, widths and cross-sections by complex scaling, Phys. Rep. **302**, 212 (1998).
[45] J. Muga, J. Palao, B. Navarro, and I. Egusquiza, Complex absorbing potentials, Phys. Rep. **395**, 357 (2004).
[46] E. C. Kemble, A Contribution to the Theory of the B. W. K. Method, Phys. Rev. **48**, 549 (1935).
[47] W. R. Sweeney, C. W. Hsu, S. Rotter, and A. D. Stone, Perfectly Absorbing Exceptional Points and Chiral Absorbers, Phys. Rev. Lett. **122**, 093901 (2019).
[48] N. T. Maitra and E. J. Heller, Semiclassical perturbation approach to quantum reflection, Phys. Rev. A **54**, 4763 (1996).
[49] M. B. Soley, K. N. Avanaki, and E. J. Heller, Reducing anomalous reflection from complex absorbing potentials: A semiclassical approach, Phys. Rev. A **103**, L041301 (2021).
[50] M. Reicherter, T. Haist, E. Wagemann, and H. J. Tiziani, Optical particle trapping with computer-generated holograms written on a liquid-crystal display, Opt. Lett. **24**, 608 (1999).
[51] D. McGloin, G. C. Spalding, H. Melville, W. Sibbett, and K. Dholakia, Applications of spatial light modulators in atom optics, Opt. Express **11**, 158 (2003).
[52] N. Mantella, J. McGowan IV, H. Neeraj, D. Spierings, and A. Steinberg, An Atomic Fabry-Perot for the Generation and Measurement of Ultracold Wavepackets, in *Proceedings of the 53rd Annual Meeting of the APS Division of Atomic, Molecular and Optical Physics*, Vol. 67, pp. F01–088, https://meetings.aps.org/Meeting/DAMOP22/Session/F01.88.
[53] K. Henderson, C. Ryu, C. MacCormick, and M. Boshier, Experimental demonstration of painting arbitrary and dynamic potentials for Bose–Einstein condensates, New J. Phys. **11**, 043030 (2009).
[54] G. Gauthier, I. Lenton, N. M. Parry, M. Baker, M. Davis, H. Rubinsztein-Dunlop, and T. Neely, Direct imaging of a digital-micromirror device for configurable microscopic optical potentials, Optica **3**, 1136 (2016).
[55] N. Navon, R. P. Smith, and Z. Hadzibabic, Quantum gases in optical boxes, Nat. Phys. **17**, 1334 (2021).
[56] D. R. Scherer, C. N. Weiler, T. W. Neely, and B. P. Anderson, Vortex Formation by Merging of Multiple Trapped Bose-Einstein Condensates, Phys. Rev. Lett. **98**, 110402 (2007).
[57] S. Bergamini, B. Darquié, M. Jones, L. Jacubowiez, A. Browaeys, and P. Grangier, Holographic generation of microtrap arrays for single atoms by use of a programmable phase modulator, J. Opt. Soc. Am. B **21**, 1889 (2004).
[58] V. Boyer, R. M. Godun, G. Smirne, D. Cassettari, C. M. Chandrashekar, A. B. Deb, Z. J. Laczik, and C. J. Foot, Dynamic manipulation of Bose-Einstein condensates with a spatial light modulator, Phys. Rev. A **73**, 031402(R) (2006).
[59] M. Pasienski and B. DeMarco, A high-accuracy algorithm for designing arbitrary holographic atom traps, Opt. Express **16**, 2176 (2008).
[60] A. L. Gaunt and Z. Hadzibabic, Robust digital holography for ultracold atom trapping, Sci. Rep. **2**, 1 (2012).